Temperature dependent lattice instability in single crystals of ferromagnetic $CdCr_2Se_4$ diluted with In and Sb

2008 J. Phys.: Condens. Matter 20 425209

(http://iopscience.iop.org/0953-8984/20/42/425209)

J. Phys.: Condens. Matter **20** (2008) 425209 (8pp) doi:10.1088/0953-8984/20/42/425209

Temperature dependent lattice instability in single crystals of ferromagnetic $CdCr_2Se_4$ diluted with In and Sb

A Waśkowska[1], L Gerward[2], J Staun Olsen[3], W Morgenroth[4], E Malicka[5] and D Skrzypek[6]

[1] Institute of Low Temperature and Structure Research, Polish Academy of Sciences, PL-50 422 Wrocław, Poland
[2] Department of Physics, Technical University of Denmark, DK-2800 Lyngby, Denmark
[3] Niels Bohr Institute, Oersted Laboratory, University of Copenhagen, DK-2100 Copenhagen, Denmark
[4] Institute of Chemistry, Aarhus University, DK-8000 Aarhus C, Denmark, c/o DESY/HASYLAB, D-22603 Hamburg, Germany
[5] Institute of Chemistry, University of Silesia, PL 40-006 Katowice, Poland
[6] Institute of Physics, University of Silesia, PL 40-007 Katowice, Poland

E-mail: A.Waskowska@int.pan.wroc.pl

Received 12 June 2008, in final form 7 August 2008
Published 25 September 2008
Online at stacks.iop.org/JPhysCM/20/425209

Abstract

In ferromagnetic $CdCr_2Se_4$ diluted with Me_x^{3+} = In and Sb, deviations from cubic symmetry $Fd\bar{3}m$ appear in the paramagnetic phase just below room temperature, and they increase with decreasing temperature. For Sb admixture, the unit-cell anomalies indicate a structural phase transition to occur at the same temperature as the magnetic transition, $T_c = 130$ K, which also is the same T_c as for the parent crystal $CdCr_2Se_4$. The low temperature phase has been described in orthorhombic space group $Fddd$. For In admixture, a structural transition occurs in the paramagnetic state at about $T_a \approx 200$ K (which is higher than $T_c = 125$ K), to a tetragonal structure with space group $I4_1/amd$. This behaviour is attributed to macroscopic spontaneous strain due to chemical heterogeneities, and to spin frustrations due to mixed valencies of Cr. The paramagnetic Curie–Weiss temperature θ_{C-W} decreases for both admixtures, indicating changes in competing ferromagnetic and antiferromagnetic interactions. The magnetization at 2.1 K exhibits saturation for $H > 0.6$ T. The magnetic moments are $\mu_{sat} = 6.26$ and 5.47 μ_B mol^{-1} for Sb and In admixtures, respectively. These values are consistent with the Cr^{3+} and Cr^{2+} mixed valencies, and with the proposed cation distribution model. A spin–phonon coupling of the transitions in the crystal with Sb admixture is suggested, while such a correspondence is not clear for the In admixture.

(Some figures in this article are in colour only in the electronic version)

Introduction

Chromium based spinel selenides are subjects of continuous interest because of their complex physical characteristics related to their ferromagnetic or ferroelastic order, and their electronic transport properties [1–5]. $CdCr_2Se_4$ is a representative of this class of compounds; it is a normal cubic spinel with space group $Fd\bar{3}m$, the Cd^{2+} ions being located at tetrahedral sites, and the magnetic Cr^{3+} ions at octahedral sites [1, 6]. The compound remains paramagnetic down to $T_c = 130$ K, below which temperature a long-range collinear ferromagnetic order appears [1, 2]. The magnetic behaviour results from a competition between the direct antiferromagnetic (AFM) Cr–Cr spin couplings and the ferromagnetic (FM) Cr–Se–Cr exchange interactions. The paramagnetic moment $\mu_{eff} = 3.8\ \mu_B$ is close to the spin-only

value of Cr^{3+}, and the paramagnetic Curie–Weiss temperature is $\theta_{C-W} = 200$ K, indicating a dominant FM coupling [1]. A number of authors have discussed the physics and chemistry of $CdCr_2Se_4$ as seen in [7] and references therein.

Lehmann and Robbins [2] have shown that $CdCr_2Se_4$ is a semiconductor, although the conductivity depends strongly on the stoichiometry. At room temperature the stoichiometric compound is an n-type semiconductor with $\sigma = 10^{-4}$ $(\Omega\ \mathrm{cm})^{-1}$, while anion vacancies in e.g. $CdCr_2Se_{3.84}$ result in p-type conductivity [4, 5]. A large negative magnetoresistance due to the mobility of the charge carriers has been observed in the ferromagnetic state [8]. Crystal structure studies close to the magnetic ordering temperature indicate inhomogeneous lattice distortions with a small shift of the anion parameter, but the symmetry does not change down to 77 K [9].

Recently, relaxor ferroelectricity and colossal magnetocapacitance have been reported for several chalcogenides, e.g. $ZnCr_2S_4$ [10], $HgCr_2S_4$ [11, 12], $CdCr_2S_4$ [13–17], and $CdCr_2Se_4$ [14]. However, the view on multiferroic properties of the spinels became a subject of sceptical and critical opinions, expressed in [18–28], where it was demonstrated that the evidence based solely on measurements of dielectric enhancement and relaxation dynamics, likewise magnetocapacitance, is not unambiguous in the case of samples which are bad insulators. The anomalies shown in [10–17] may equally appear without true magnetoelectric coupling, being simple conductivity artefacts [18–25]. There are a range of physical, electronic and symmetry properties limiting ferromagnetic and ferroelectric coexistence [26–28]. Crucial experiments establishing a possible control of magnetic ordering on polar atomic displacements in centrosymmetric $CdCr_2Se_4$ have not been performed yet. An obvious difficulty lies in the semiconducting properties of this ferromagnet, which will not endure the electric fields necessary for switching polarization.

The spinel structure easily forms substitutional solid solutions. Various divalent or trivalent admixture ions may be distributed between the tetrahedral or octahedral anion sites in the cubic structure, resulting in numerous modifications of the magnetic and electronic transport characteristics [29–32]. Continuing our investigations on ferroic properties of the chalcogenides, we have prepared single crystals of $CdCr_2Se_4$ admixed with nonmagnetic Me_x^{3+} = In and Sb. One of the aims is to study the temperature dependent structural stability in the range 100–300 K and relate it to static magnetic characteristics of spinels containing isovalent Me^{3+} of different ionic radii (in the octahedral coordination $R = 0.76$ and 0.81 Å for Sb^{3+} and In^{3+}, respectively) [33]. These quaternary solid solutions allow for testing different magnetic and lattice interactions. In the present paper, we report a detailed analysis of the evolution of the crystal lattice distortions for decreasing temperature. High resolution x-ray diffraction data at low temperatures have been obtained with a four-circle diffractometer using synchrotron radiation. In addition, we have made comparative crystal structure determinations at 105 K and room temperature using a single-crystal diffractometer and a laboratory x-ray source. The results are related to the magnetic susceptibility and saturation behaviour of the two types of admixture.

1. Experimental details

Single crystals of $CdCr_2Se_4$ spinel diluted with Me_x^{3+} = In, Sb were grown from binary selenides CdSe, Sb_2Se_3 and In_2Se_3 by the chemical transport method with $CrCl_3$ as the transport agent. The method has been described in detail elsewhere [34]. The presence of antimony or indium in the single crystals was tested by means of energy-dispersive x-ray fluorescence (XRF), using the standardless fundamental parameters method, and by means of wavelength-dispersive x-ray fluorescence (WDXRF), using a sequential spectrometer Philips PW1410. Compositional analysis was based on a crystal structure determination using an x-ray diffraction technique.

The temperature dependence of the unit-cell parameters was measured at station D3 of the Hamburg Synchrotron Radiation Laboratory (HASYLAB), using a Huber four-circle diffractometer. The wavelength was adjusted to $\lambda = 0.7000$ Å. Low temperatures in the range 100–300 K were obtained using an Oxford Cryojet based on liquid nitrogen. At each temperature, the unit-cell dimensions were calculated by a least-squares refinement using the setting angles of 24 high angle Bragg reflections with $2\theta \approx 75°$. The sample was given 15 min for reaching thermal equilibrium before the measurement.

Crystal structure determinations at 300 and 105 K were performed with graphite monochromated Mo Kα radiation using a KM-4 *Xcalibur* single-crystal diffractometer (Oxford Diffraction). The instrument was operating in the κ geometry and equipped with a CCD detector. The data were collected in ω-scan mode with $\Delta\omega = 1.2°$. About 1000 images were recorded in nine runs with different angular settings, covering 99% and 91% of the Ewald sphere at 300 and 105 K, respectively. The diffraction data were integrated for intensities and corrected for Lorentz polarization effects using the *CrysAlis* program package [35]. Structure calculations based on F^2 data were made with the *SHELXL97* program system [36].

Magnetic susceptibility and low field (1 kOe) magnetization measurements were performed in the temperature range 1.5–400 K with a Quantum Design SQUID magnetometer. The measurements were carried out without sample orientation. The experimental values of the susceptibility were corrected for a diamagnetic contribution. Saturation magnetization at high magnetic fields was measured with a Faraday-type Cahn RG automatic electro-balance at 2.1 K in an external field up to 70 kOe.

2. Experimental results

2.1. Crystal structure and cation distribution at room temperature

We find that the admixtures of In and Sb in $CdCr_2Se_4$ crystals do not break the cubic symmetry at room temperature. From earlier investigations of quaternary spinels it has been found that Sb and In can accommodate at both A sites (tetrahedral voids) and at B sites (octahedral voids) in the anion sublattice [19–22]. Therefore, a chemical ordering of the cations in the noncentrosymmetric space group $F\bar{4}3m$

Table 1. Crystal data, experimental details and structure refinement for $CdCr_2Se_4$:Me^{3+} = Sb, In at room temperature.

Crystal data	$(Cd_{0.75}Sb_{0.25})[Cr_2]Se_4$	$(Cd_{0.73}In_{0.27})[Cr_{1.88}In_{0.12}]Se_4$
Crystal system, space group	Cubic, $Fd\bar{3}m$	Cubic, $Fd\bar{3}m$
Unit-cell dimensions (Å): a	10.746 4(13)	10.757 5(18)
Volume (Å^3)	1241.05(3)	1244.92(3)
Z; calculated density (Mg m^{-3})	8; 5.722	8; 5.767
Crystal size (mm)	0.12 × 0.10 × 0.09	0.13 × 0.10 × 0.08
Data collection		
Wavelength (Å)	0.710 73	0.710 73
$2\theta_{max}$ for data collection	90.35	90.23
Limiting indices: h	− 15, 21	− 21, 15
k	− 9, 21	− 13, 19
l	− 20, 15	− 21, 21
Reflections collected	6345	6522
Reflections unique	289	289
Reflections ($I > 2\sigma(I)$)	251	257
Absorption coefficient (mm^{-1})	30.39	30.56
Absorption correction	Numerical	Numerical
R_{int} before and after abs. correction	0.127, 0.052	0.143, 0.055
Refinement		
Goodness of fit on F^2	1.009	1.010
Final R indices ($I > 2\sigma(I)$) R_1	0.025	0.020
wR_2	0.068	0.045
Extinction coefficient	0.003 6(2)	0.001 09(50)
Largest diff. peak and hole (eÅ^{-3})	1.49 and −1.95	0.88 and −0.94

Table 2. Atomic positions for $(Cd_{0.75}Sb_{0.25})[Cr_2]Se_4$ and $(Cd_{0.73}In_{0.27})[Cr_{1.88}In_{0.12}]Se_4$ at room temperature in $Fd\bar{3}m$. The isotropic displacement parameters U_{iso} (in Å^2 × 10^3) are given for the cations, and $U_{eq} = (1/3)\Sigma_i\Sigma_j U_{ij}a_i^*b_j^*\mathbf{a}_i\mathbf{a}_j$ is for the Se ion.

Compound	Anion positional parameter u	SOF (A) site	SOF [B] site	U_{iso}/U_{eq} (Å^2 × 10^3) (A) site	[B] site	Se
$(Cd_{0.75}Sb_{0.25})[Cr_2]Se_4$	0.264 21(3)	0.746(2)/0.25	1.0	9.2(2)	5.4(2)	5.9(2)
$(Cd_{0.73}In_{0.27})[Cr_{1.88}In_{0.12}]Se_4$	0.263 97(2)	0.728(4)/0.27	0.936(2)/0.06	11.4(1)	9.3(2)	8.23(9)

The atomic positions:
(A) site: 8a (1/8, 1/8, 1/8); [B] site: 16d (1/2, 1/2, 1/2); and the anion site: 32e (u, u, u).

was considered in connection with possible ordering or aggregation phenomena, in addition to the order–disorder location of the admixtures in the centrosymmetric space group $Fd\bar{3}m$ (No 227). The space group $F\bar{4}3m$ would allow the crystallographically distinct tetrahedral 4a and 4c positions for Cd^{2+} and Me^{3+}, and the 16e site for Cr^{3+}. The space groups $Fd\bar{3}m$ and $F\bar{4}3m$ can be discriminated by the $\{hk0\}$-type reflections with $h + k = 4n + 2$. These reflections are systematically extinct in $Fd\bar{3}m$ but allowed in $F\bar{4}3m$.

An evident absence of the $\{hk0\}$-type reflections with $h + k = 4n + 2$ in the experimental set has ruled out the lower symmetry. The diffraction data were therefore analysed in the conventional space group $Fd\bar{3}m$ (No 227) with refined site occupation factors (SOF) for both (A) and [B] sites. The best refinement corresponds to mixed order–disorder Cd/Sb occupancy at the (A) site, leading to the following chemical composition: $(Cd_{0.75}Sb_{0.25})[Cr_2]Se_4$. Crystal data, experimental details and the structure refinement for this sample are given in table 1.

Indium admixture was found in both (A) and [B] sites, and as for the former crystal no indication for cation ordering could be observed. Thus, the formula obtained for this compound is $(Cd_{0.73}In_{0.27})[Cr_{1.88}In_{0.12}]Se_4$.

Table 3. Selected distances (in Å) and angles (in deg) for$(Cd_{0.75}Sb_{0.25})[Cr_2]Se_4$ and $(Cd_{0.73}In_{0.27})[Cr_{1.88}In_{0.12}]Se_4$ at room temperature in $Fd\bar{3}m$.

Atoms	$(Cd_{0.75}Sb_{0.25})[Cr_2]Se_4$	$(Cd_{0.73}In_{0.27})[Cr_{1.88}In_{0.12}]Se_4$
(A)–Se	2.591 2(6) 4×	2.589 4(6) 4×
[B]–Se	2.543 0(4) 6×	2.548 0(5) 4×
Cr–Cr	3.799 4(4) 6×	3.803 4(7) 6×
Se–(A)–Se	109.47(0)	109.47(0)
(A)–Se–[B]	120.39(1) 3×	120.48(1) 3×
Cr–Se–Cr	96.67(1) 3×	96.55(1) 3×
Se–[B]–Se	97.08(1) 6×	96.95(1) 6×

Atomic coordinates, site occupation factors and thermal displacement parameters are given in table 2. The static positional disorder has some influence on the thermal displacement amplitudes, which for sites with mixed occupancy are higher than for the Se atom. Selected geometric parameters for the two crystals are shown in table 3.

2.2. Thermal expansion

The temperature dependent evolution of the unit-cell dimensions for $(Cd_{0.75}Sb_{0.25})Cr_2Se_4$ is shown in figure 1. At

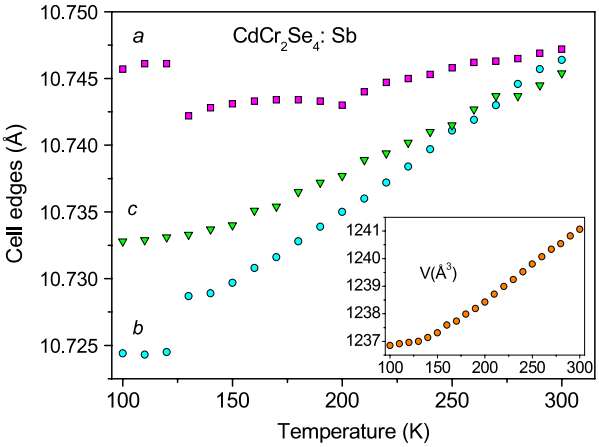

Figure 1. Evolution of the unit-cell dimensions of $Cd_{0.75}Sb_{0.25}[Cr_2]Se_4$ for decreasing temperature. The inset shows the unit-cell volume as a function of temperature (magnetostriction).

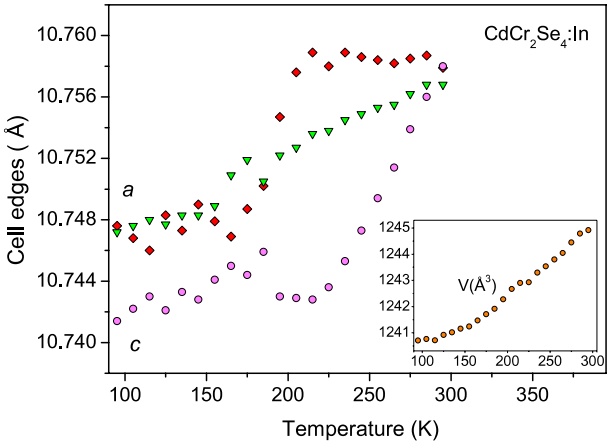

Figure 2. Evolution of the unit-cell dimensions of $(Cd_{0.73}In_{027})[Cr_{1.88}In_{0.12}]Se_4$. The large scatter of the data points reflects the cluster structure of the crystal. The inset shows the unit-cell volume as a function of temperature.

room temperature (RT) the cell dimensions agree exactly with the cubic cell and they do not differ from those of the parent crystal, $CdCr_2Se_4$, owing to the similarity of the Cd and Sb ionic radii at the tetrahedral sites (0.78 and 0.76 Å, respectively). However, with decreasing temperature a systematic deviation from cubic symmetry is observed in the paramagnetic phase. The effect has features of elastic strain, which develops progressively down to T_c. The standard deviation, 0.0013 Å at 300 K, increases systematically due to the broadening of the reflections, reaching 0.0035 Å at 100 K. Close to T_c there is a small but clear structural transition to an orthorhombic structure. The ferromagnetic long-range ordering, which takes place at this temperature, is accompanied with a magnetostriction effect, as seen in the critical region of the volume–temperature dependence (inset in figure 1).

Strong fluctuations of the unit-cell dimensions, in particular for the In-admixed sample $(Cd_{0.73}In_{0.27})[Cr_{1.88}In_{0.12}]$ in figure 2, typically indicate cluster structure due to variations in the cation distribution. The standard deviations (0.0018 Å at 300 K, and 0.0035 Å at 105 K) are slightly larger than for the Sb-admixed crystal. The random location of two different cations at both (A) and [B] sites leads to chemically different bonds. The sample with such chemical heterogeneities may reach thermodynamical equilibrium when quenched from high temperature to RT, and its structure can therefore be described by cubic symmetry. The chemical composition, however, produces fine-scale cracks or clusters with size typically in the range 100–200 Å [28]. Clusters with different local distortions may be pinned by e.g. strain, ionic vacancies or short-range polar and magnetic interactions. When the temperature is decreased, the fluctuations in these factors can cause the interactions between the clusters leading to geometrical frustration, and at about $T_a \approx 200$ K the crystal relieves of the frustration by lowering symmetry. Condensation of the clusters results in a monodomain state and long-range order. In the present experiment, however, domains of different volumes remain even below T_a. Therefore, the overall tetragonal cell should be treated as averaged over those domains. Their presence is evident from the scatter of the data points in the low temperature range (figure 2).

2.3. X-ray crystal structures at 105 K

If the crystal is cooled through T_c in the absence of any external magnetic or strain field, there are two possible choices for each of the three cubic axes to transform into the orthorhombic a, b or c axes. The most general situation is then a multiple-twinned structure, i.e. a mosaic of single crystals with different axial combinations. The crystal in such a state will have isotropic properties, which are different, however, from those at room temperature. In the present experiment, the twinning averages the changes resulting from the observed phase transition.

On the basis of the unit-cell behaviour, the low temperature (LT) crystal structure of $(Cd_{0.75}Sb_{0.25})[Cr_2]Se_4$ has been determined at 105 K, assuming an orthorhombic structure with space group $Fddd$ (No 70). We could not observe either superstructure reflections or essential diffuse scattering. The refinement converged well, but the departures from the cubic symmetry are not larger than two to three standard deviations, mirroring the average of the polydomain state. Experimental and structure calculation details are collected in tables 4 and 5. Selected bond distances and angles are given in table 6. The lower than cubic symmetry originates from a distortion in the $CrSe_6$ octahedra, exhibiting three pairs of different Cr–Se bonds, while the uniformly compressed (A) sites remain regular tetrahedra. There are no essential changes in (A)–Se–[B] and octahedral angles, which could point to the polyhedral tilting.

The crystal structure of $(Cd_{0.73}In_{0.27})[Cr_{1.88}In_{0.12}]$ at 105 K has been refined in space group $I4_1/amd$ (No 141). The tetragonal deformation is given by the ratio $c/a = 0.9996$. Also, in this compound, the symmetry decrease is connected with strain relaxation, resulting in a small distortion of the [B] sites. The transition temperature, here $T_a \approx 200$ K, depends however on the sample. The octahedral sites are

Table 4. Crystal data, experimental details and structure refinement for $CdCr_2Se_4$:Me^{3+} = Sb, In at 105 K.

Crystal data	$(Cd_{0.75}Sb_{0.25})[Cr_2]Se_4$	$(Cd_{0.73}In_{0.27})[Cr_{1.88}In_{0.12}]Se_4$
Crystal system, space group	Orthorhombic, $Fddd$	Tetragonal, $I4_1/amd$
Unit-cell dimensions (Å) a	10.746(3)	7.599(3)
b	10.724(3)	7.599(3)
c	10.733(3)	10.742(3)
Volume(Å^3)	1236.87(6)	620.29(3)
Z; Calc. density (Mg m^{-3})	8; 5.741	4; 5.787
Data collection		
Wavelength (Å)	0.710 73	0.710 73
$2\theta_{max}$ for data collection	87.41	87.36
Limiting indices: h	− 19, 13	− 11, 14
k	− 14, 20	− 14, 14
l	− 20, 19	− 11, 20
Reflections collected	5317	5499
Reflections unique	1087	653
Reflections ($I > 2\sigma(I)$)	1005	546
R_{int} before and after abs. correction	0.130; 0.054	0.143, 0.053
Refinement		
Goodness of fit on F^2	1.008	1.002
Final R indices ($I > 2\sigma(I)$) R_1	0.033	0.021
wR_2	0.068	0.044
Extinction coefficient	0.0026(1)	0.0031(1)
Largest diff. peak and hole (eÅ^{-3})	2.58 and −2.25	1.58 and −1.91

Table 5. Fractional atomic coordinates and thermal displacement amplitudes U_{iso} (in Å^2 × 10^3) for $(Cd_{0.75}Sb_{0.25})[Cr_2]Se_4$ and $(Cd_{0.73}In_{0.27})[Cr_{1.88}In_{0.12}]Se_4$ at 105 K.

$(Cd_{0.75}Sb_{0.25})[Cr_2]Se_4$ in $Fddd$ (origin choice 2).					
Atom	Wyckoff position	U_{iso}			
Cd/Sb	8a (1/8, 1/8, 1/8)	4.08(11)			
Cr	16d (1/2, 1/2, 1/2)	3.09(12)			
Se	32h (x, y, z)	3.08(10)			
$x = 0.264\,27(2)$, $y = 0.264\,40(2)$, $z = 0.264\,30(2)$					
$(Cd_{0.73}In_{0.27})[Cr_{1.88}In_{0.12}]Se_4$ in $I4_1/amd$ (origin choice 2).					
Atom	Wyckoff position	x	y	z	U_{iso}
Cd/In	4b	0	0.25	0.375	3.80(7)
Cr/In	8c	0	0.5	0	3.75(14)
Se	16h	0	0.528 08(3)	0.235 60(2)	3.01(6)

Table 6. Selected distances (in Å) and angles (in deg) for $(Cd_{0.75}Sb_{0.25})[Cr_2]Se_4$ and $(Cd_{0.73}In_{0.27})[Cr_{1.88}In_{0.12}]Se_4$ at 105 K.

Atoms	$(Cd_{0.75}Sb_{0.25})[Cr_2]Se_4$ in $Fddd$	$(Cd_{0.73}In_{0.27})[Cr_{1.88}In_{0.12}]Se_4$ in $I4_1/amd$
(A)–Se	2.590 3(9) 4×	2.589 9(8) 4×
[B]–Se	2.535 9(8) 2×	2.539 8(7) 2×
[B]–Se	2.539 1(8) 2×	2.544 9(9) 4×
[B]–Se	2.542 5(9) 2×	—
Cr–Cr	3.793(1) 6×	3.798 7(9) 6×
Se–(A)–Se	109.36(3), 109.50, 109.55	109.36(1), 109.53(1)
(A)–Se–[B]	120.33(3), 120.34, 120.38	120.37(1), 120.50(2)
Cr–Se–Cr	96.70(3) 1×, 96.73(3) 2×	96.57(1) 3×, 96.67(1) 3×
Se–[Cr]–Se	97.12(3) 2×, 97.15(3) 4×	97.08(1) 6×

axially compressed, two of the [B]–Se bonds being shorter (table 6). We consider this distortion as a preparatory stage for the magnetic transition at the lower temperature T_c = 125 K.

2.4. Magnetic measurements

The dc magnetic susceptibility, $\chi(T)$, and its inverse, $\chi^{-1}(T)$, in an applied magnetic field of 1 kOe are shown in figures 3 and 4 as functions of temperature for $(Cd_{0.75}Sb_{0.25})[Cr_2]Se_4$ and $(Cd_{0.73}In_{0.27})[Cr_{1.88}In_{0.12}]$, respectively. For both compounds, the ferromagnetic transition temperature, T_c, was estimated from the inflection point in susceptibility $\chi(T)$ using the maximum slope, $d\chi/dT$. The paramagnetic Curie–Weiss temperature θ_{C-W} and the magnetic moment μ_{eff} were estimated from the Curie–Weiss law, which is fulfilled for $T > 270$ K. The field dependent magnetic moments are shown in figure 5. The saturation magnetization occurs at a relatively low field. For $(Cd_{0.75}Sb_{0.25})[Cr_2]Se_4$ the saturation magnetization $\mu_{sat} = 6.25\ \mu_B$ mol^{-1} is larger than for pure $CdCr_2Se_4$ where $\mu_{sat} = 5.78$–$6.0\ \mu_B$ mol^{-1}, and this feature will be discussed below. The saturation magnetic moment is much lower, $\mu_{sat} = 5.47\ \mu_B$ mol^{-1},

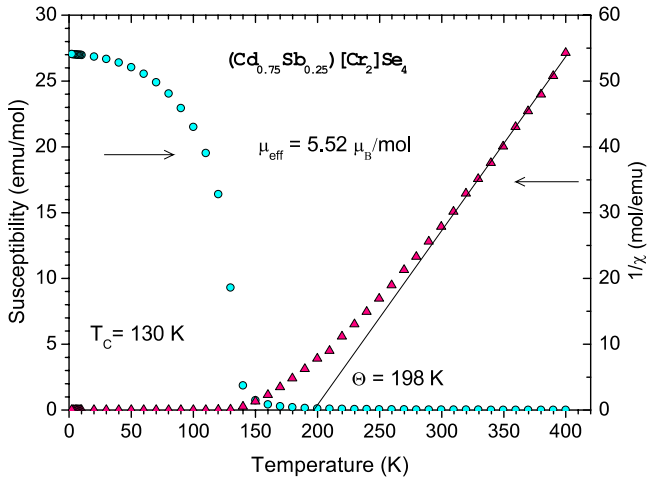

Figure 3. Magnetic susceptibility and its inverse for $(Cd_{0.75}Sb_{025})[Cr_8]Se_4$ as functions of temperature.

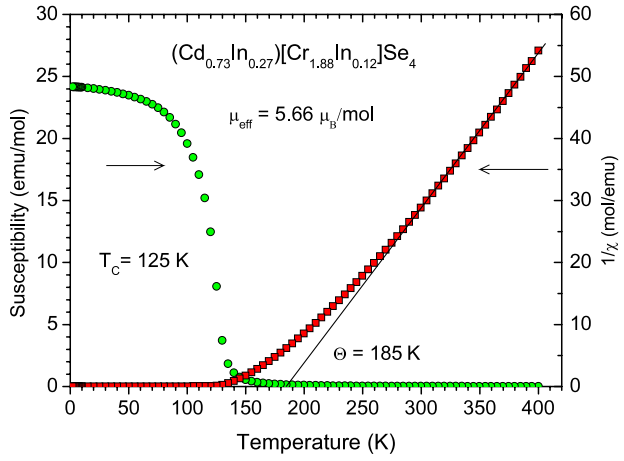

Figure 4. Magnetic susceptibility and its inverse for $(Cd_{0.73}In_{027})[Cr_{1.88}In_{0.12}]Se_4$ as functions of temperature.

for $(Cd_{0.73}In_{0.27})[Cr_{1.88}In_{0.12}]Se_4$ with a diluted chromium sublattice.

3. Discussion

Dilutions of the $CdCr_2Se_4$ structure with Sb and In do not break the cubic symmetry at room temperature (RT). The unit-cell dimension of $(Cd_{0.75}Sb_{0.25})Cr_2Se_4$ is nearly the same as for the parent crystal $CdCr_2Se_4$. However, it is interesting to note that the initially negligible number of orthorhombic domains which may be present at RT increases at the cost of the cubic domains with decreasing temperature. The process has a dynamical character, in contrast to the static phase transition at T_c. Such a behaviour may originate from the electronic state of the Cr ions.

A charge neutrality of the sample requires compensation of the $(Cd^{2+}Sb^{3+})$ pseudo-ion at the (A) sites. Thus, an equivalent number of Cr^{2+} ions must be generated at the [B] sites and, consequently, the cation distribution should be written as $(Cd^{2+}_{0.75}Sb^{3+}_{0.25})[Cr^{3+}_{1.75}Cr^{2+}_{0.25}]Se_4$. The Cr^{3+} ions with

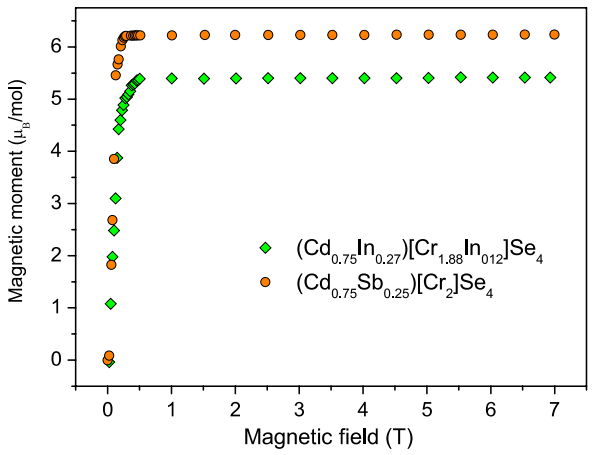

Figure 5. Magnetization curves for $(Cd_{0.73}In_{027})[Cr_{1.88}In_{0.12}]Se_4$ and $(Cd_{0.75}Sb_{025})[Cr_8]Se_4$.

half-filled t_{2g} orbitals ($S = 3/2$) are not Jahn–Teller active, while the Cr^{2+} ions with a $3d^4$ electron configuration are Jahn–Teller ions. The latter form distorted $Cr^{2+}Se_6$ octahedra, with two shorter bonds giving rise to strains of ferroelastic nature in the paramagnetic phase.

The mixed Cr valences also bring about some spin frustration due to the fluctuations of the crystal field about Cr^{3+} and Cr^{2+}. Therefore, the variation of the unit-cell dimensions in the paramagnetic phase (figures 1 and 2) can be interpreted in terms of the local atomic configuration and coupled spin fluctuations within the structural domains. The size of the domains increases with decreasing temperature. Close to T_c the structure relaxes by lowering its macroscopic symmetry to orthorhombic. Thus, the development of the spontaneous strain is linked with the magnetic ordering, because both phenomena are driven by the electronic properties of the chromium ions.

In $(Cd_{0.73}In_{0.27})[Cr_{1.88}In_{0.12}]Se_4$, the spin heterogeneity at the octahedral sites is additionally enhanced by dilution with In ions and the resulting bond frustration. The strain driven transition at T_a has no clear relationship to the magnetic transition at T_c ($T_a > T_c$), although the former may be considered as a preparatory stage for the spin ordering at $T_c = 125$ K. As observed in a sample with a similar In^{3+} distribution [22], the local distortions above T_c are evident from EPR line broadening in the paramagnetic phase. These effects have made some impact not only on the paramagnetic Curie–Weiss temperature, which is $\theta_{C-W} = 185$ K, but also on the molar magnetic saturation $\mu_{sat} = 5.47\ \mu_B\ mol^{-1}$, which is lower than in the parent crystal $CdCr_2Se_4$. This means that part of the Cr–Se–Cr exchange path is not present because of the order–disorder distribution of nonmagnetic indium at the [B] sites. Obviously, also some of the higher order neighbours forming the (n–n–n) superexchange couplings of the type Cr–Se–Cd/In–Se–Cr must have become perturbed.

Comparing the important interatomic distances and angles, there is no appreciable change in the average geometry of the RT and LT phases. However, it can be noted that while the (A)–Se bond lengths are nearly the same in the two phases, the octahedral sites are compressed at LT. The magnetic ordering depends on, among other factors, the

distance between the Cr ions at octahedral sites, as well as on the Se separations in the anion sublattice, due to Cr–Se–Cr exchange. The magnetic interactions are thus stronger for shorter [B]–Se distances.

Magnetic characteristics in figures 3 and 4 show that in both systems the inverse susceptibility $\chi^{-1}(T)$ follows the Curie–Weiss law only in the range 270–400 K. Below 270 K, the curves deviate from the straight line, indicating strong spin fluctuations and progressively increasing short-range ordering. This tendency is consistent with the results of the crystal structure determinations, which suggest that the mixed chromium ion valence state at the [B] sites and structural distortions enhance the role of electronic correlations.

4. Conclusions

(1) The present compounds have in common the fact that the onset of ferromagnetic ordering is accompanied by small ferroelastic distortions, hardly detectable from standard x-ray diffraction. Using high resolution synchrotron x-ray data for Sb-substituted $CdCr_2Se_4$, we are able to observe the structural dynamics connected with spin frustration in the paramagnetic phase, and a spin–phonon coupled phase transition at a temperature close to the magnetically ordered state at T_c. In the In-substituted compound, the admixture causes elastic strain, which propagates through the crystal and lowers its symmetry at $T_a > T_c$. The low temperature phase can be considered a preparatory stage for the ferromagnetic ordering at $T_c = 125$ K.

(2) The centrosymmetric space groups ascribed to the LT phases, being subgroups of prototype $Fd\bar{3}m$, permit ferroelasticity but exclude ferroelectric polarization [26–28]. This feature of the crystals is consistent with the view concerning their multiferroic nature and published in [18–28]. Since the compounds are bad insulators, one of the likely factors inhibiting ferroelectric order may be the charge transfer between Cr^{3+} and Cr^{2+} ions. It is experimentally proven for perovskite-like compounds that d orbital occupancy, rather then d electron magnetism is crucial to the ferroelectric distortion cancellation [27, 37, 38].

(3) As the temperature is decreased from RT, deviations from the Curie–Weiss law can be observed in both compounds. This behaviour points to a progressively increasing collective interactions between the clusters and correlates well with the temperature dependent behaviour of the unit-cell dimensions.

(4) Compared to the case for pure $CdCr_2Se_4$, the tetrahedral location of the Sb^{3+} admixture has a small impact on $T_c = 130$ K and the paramagnetic Curie–Weiss temperature $\theta_{C-W} = 198$ K. There is however, a small magnetization increase, which we relate to changes in the number of competing ferromagnetic and antiferromagnetic interactions due to the mixed chromium valencies. A decrease in magnetization takes place in the sample with In admixture, which enhances the disorder because of the location of indium in the $CrSe_6$ sublattice.

(5) This study demonstrates a quantitative relation between the random structure distortion caused by the chemical substitution, and the dynamics of the elastic behaviour induced by the development of the magnetic order in CdCr2Se:Me^{3+}. There is a need for more extensive studies by means of neutron and electron diffraction to evidence the geometric spin frustration. These, combined with field frequency dependent dynamic magnetic and dielectric properties, could throw more light on the relaxational nature of the reported phenomena. However, conclusive experiments proving the nature of temperature dependent anomalies would require samples being magnetically, electrically and mechanically *true* single domains. We speculate that the randomness existing in real crystal modifies the critical behaviour from that in ideal single-domain counterpart.

Acknowledgments

The authors wish to thank HASYLAB/DESY in Hamburg, Germany, for permission to use the synchrotron radiation facility. LG and JSO gratefully acknowledge financial support from the Danish Natural Sciences Foundation through DANSYNC.

References

[1] Balzer P, Wojtowicz P J, Robbins M and Lopatin E 1966 *Phys. Rev.* **151** 367–77
[2] Lehmann H W and Robbins M 1966 *J. Appl. Phys.* **37** 1389–90
[3] Pinch H L and Berger S 1968 *J. Phys. Chem. Solids* **29** 2091–99
[4] Amith A and Friedman L 1970 *Phys. Rev.* B **2** 434–5
[5] Groń T, Krajewski A, Kusz J, Malicka E, Okońska-Kozlowska I and Waśkowska A 2005 *Phys. Rev.* B **71** 035208
[6] Borovskaya T N, Butman L A, Tsirelson V G, Poray-Koshits M A, Aminov T G and Ozerov R P 1991 *Kristallografiya* **36** 612–6
[7] Kalinnikov V T, Aminov T G and Novotvortsev V M 2003 *Inorg. Mater.* **39** 997–1012
[8] Martin W, Kellogg A T, White R L, White R M and Pinch H 1969 *J. Appl. Phys.* **40** 1015–6
[9] Göbel H 1976 *J. Magn. Magn. Mater.* **3** 143–6
[10] Rudolf T, Kant Ch, Mayr F, Hemberger J, Tsurkan V and Loidl A 2007 *Phys. Rev.* B **75** 052410
[11] Rudolf T, Kant Ch, Mayr F, Hemberger J, Tsurkan V and Loidl A 2007 *Phys. Rev.* B **76** 174307
[12] Tsurkan V, Hemberger J, Krimmel A, Krug von Nidda H-A, Lunkenheimer P, Weber S, Zestra V and Loidl A 2006 *Phys. Rev.* B **73** 224442
[13] Fritsch V, Hemberger J, Buttgen N, Scheidt E-W, Krug von Nidda H-A, Loidl A and Tsurkan V 2004 *Phys. Rev. Lett.* **92** 116401
[14] Hemberger J, Lunkenheimer P, Fichtl R, Weber S, Tsurkan V and Loidl A 2005 *Nature* **434** 364–7
[15] Lunkenheimer P, Fichtl R, Hemberger J, Tsurkan V and Loidl A 2005 *Phys. Rev.* B. **72** 060103
[16] Weber S, Lunkenheimer P, Fichtl R, Krug von Nidda H-A, Tsurkan V and Loidl A 2006 *Phys. Rev. Lett.* **96** 157202
[17] Hemberger J, Lunkenheimer P, Ficht R, Weber S, Tsurkan V and Loidl A 2006 *Phase Transit.* **79** 1065–82
[18] O'Neil D, Bowman R M and Gregg J M 2000 *Appl. Phys. Lett.* **77** 1520–22
[19] Catalan G and Scott J F 2007 *Nature* **448** E4–5

[20] Hemberger J, Lunkenheimer P, Fichtl R, Krug von Nidda H-A, Tsurkan V and Loidl A 2007 *Nature* **448** E5–6
[21] Catalan G, O'Neil D, Bowman R M and Gregg J M 2000 *Appl. Phys. Lett.* **77** 3078–80
[22] Pintille L and Alexe M 2005 *Appl. Phys. Lett.* **87** 112903
[23] Catalan G 2006 *Appl. Phys. Lett.* **88** 102902
[24] Scott J F 2007 *J. Mater. Res.* **22** 2053–62
[25] Scott J F 2008 *J. Phys.: Condens. Matter* **20** 021001
[26] Hur N, Park S, Sharma P A, Ahn J S, Guha S and Cheong S-W 2004 *Nature* **429** 392–5
[27] Hill N A 2000 *J. Phys. Chem.* B **104** 6694–709
[28] Schmid H and Ascher E 1974 *J. Phys. C: Solid State Phys.* **7** 2697–06
[29] Belov K P, Koroleva L I, Shalimova M A, Kalinnikov V T and Aminov T G 1977 *Zh. Eksp. Teor. Fiz.* **72** 1994–9
[30] Nogues H, Saifi A, Hamedoun M, Dormann J L, Malmanche A, Fiorani D and Viticole S 1982 *J. Appl. Phys.* **53** 7699–701
[31] Shabunina G G, Sadykov R A and Aminov T G 2000 *Neorg. Mater.* **36** 1438–42
[32] Skrzypek D, Malicka E, Waśkowska A, Widuch S, Cichoń A and Mydlarz T 2006 *J. Cryst. Growth* **297** 419–25
[33] Shannon R D 1976 *Acta Crystallogr.* A **32** 751–67
[34] Malicka E, Waśkowska A, Mydlarz T and Kaczorowski D 2007 *J. Alloys Compounds* **440** 1–7
[35] CrysAlis CCD and CrysAlis RED 2007 Program package for data collection and data reduction *Version 1.171.32.6.* Oxford Diffraction Ltd Wrocław, Poland
[36] Sheldrick G M 2008 *SHELXL97 Acta Crystallogr.* A **64** 112–22
[37] Mizokawa T, Khomski D I and Sawatzky G A 1999 *Phys. Rev.* B **60** 7309–13
[38] Eerenstein W, Morrison F D, Scott J F and Mathur N D 2005 *Appl. Phys. Lett.* **87** 101906